Extension and Parameter Calibration of a Multi-Lane Vehicular Traffic Simulation Model

Minjie Chen[1], Günter Bärwolff[2], and Hartmut Schwandt[1]

[1] MA 6-4, Institut für Mathematik, Technische Universität Berlin
[2] MA 4-5, Institut für Mathematik, Technische Universität Berlin
Straße des 17. Juni 136, 10623 Berlin, Germany
{minjie.chen,baerwolff,schwandt}@math.tu-berlin.de

Abstract. We presented a deductive model for multi-lane vehicular traffic simulation in [1]. In the current text, variable safety distance policy is added to the previous model; in addition, we give a detailed parameter calibration. As a result, fundamental diagram close to empirical studies can be reproduced. The original model was devised for both asymmetric and symmetric traffic systems. Our test result shows very similar overall density-flow relationships in both systems.

Keywords: vehicular traffic simulation, multi-lane vehicular traffic, fundamental diagram

1 Introduction

The study of vehicular traffic serves the purpose of optimal utilization of road resources for transportation as well as enhanced safety consideration of such activities. Various simulation models have been applied for design, planning and condition prediction of real-world traffic systems. Basically, there are two categories in the modelling and simulation. Macroscopic methods concentrate on the overall system dynamics. In comparison, microscopic methods focus on the individual objects in the system which are often named "agent"s (see [4] for an overview). In the latter category, car-following models study the problem from a perspective of *individual* vehicles under the active control of their drivers; state equilibrium and numerical integration of these individual units are applied in the description of system dynamics (see the discussion in [8]). [5] introduced the first application of cellular automaton (CA) in microscopic modelling of single-lane traffic systems. In this model, discrete positions (also called "site"s) on the lanes resemble the "cell"s in the context of a CA; the system dynamics can be thus described by the state transition of *all* the cells in the simulation system. With x and v denoting position and speed of the vehicles respectively, every vehicle is

subject to a set of four simple transition rules:

$$v \Leftarrow \min(v + 1, v_{\max}), \tag{1a}$$

$$v \Leftarrow \min(x' - x - 1, v), \tag{1b}$$

$$v \Leftarrow \max(0, v - 1), \text{executed with a given probability}, \tag{2}$$

$$x \Leftarrow x + v. \tag{3}$$

The superscript $'$, as seen in (1b), is used to denote a vehicle's immediate neighbour (the leader of the current vehicle) in the flow direction. Let x' denote the position of the leading vehicle. (1a) describes the possible acceleration of the current vehicle. In comparison, (1b) shows the maximum possible position transition without risk of collision with the leading vehicle ahead. The final position transition of this vehicle is given in (3). The rule of (2) is introduced as a stochastic element; it reflects the random "dawdling" behaviour of the drivers which most of them are unaware of. Without this element, the simulation would become deterministic. A simulation cycle consists of application of these four rules on all vehicles in the system. In the original model [5] and many of its extensions (for example, the two-lane extension [7]) each site in the traffic lane has a length of 7.5 m; this value has been selected to be slightly larger than the length of an average passenger vehicle. The simulation cycle has a time length $\Delta t = 1\,\text{s}$, with this, a discrete maximum speed $v_{\max} = 5$ renders a maximum physical speed of $135\,\text{km} \cdot \text{h}^{-1}$.

2 A Deductive Multi-lane Model
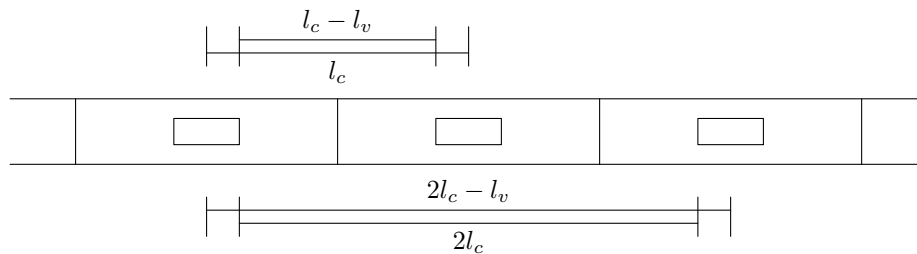
Fig. 1. Real distance between vehicles (drawn as small rectangles) in the traffic lane. The collision-free distance between two vehicles at adjacent sites (drawn as enclosing rectangles) is $l_c - l_v$ (instead of l_c or 0); the collision-free distance of a vehicle to another one at position d sites away is $d \cdot l_c - l_v$. The flow direction in the current text is always from left to right in the horizontal axis.

We presented a generalized model for vehicular traffic with multiple lanes [1]. We consider this model to be *deductive* (according to the definition of [3]), since system parameters are derived from known physical quantities. We explain this model briefly.

2.1 System Settings

In our model, safety distance will play a significant role, so first we take a closer look of the distance between the vehicles. The traffic lane will be divided into sites with an equal length l_c. Let l_v denote the average length of a typical vehicle. The collision-free distance of two vehicles at the x-th site and the $(x+d)$-th site would be $d \cdot l_c - l_v$, cf. Fig. 1. A very realistic estimate for an average passenger car would be $l_v = 5$ m. Respecting this measurement and the site length $l_c = 7.5$ m, it is almost for sure that in the model of [5] the distance between the vehicles is too small.

We start with $l_c = 15$ m and $\Delta t = 2.4$ s. In this case, position change of one site in the lane in each simulation cycle refers to a temporary speed of 22.5 km $\cdot$ h^{-1}, whereas the speed change (acceleration) is 9.375 km $\cdot$ h^{-1} every second (approximately eleven seconds from 0 to 100 km $\cdot$ h^{-1}), which resembles the capacity of an average modern passenger car.

2.2 Safety distance

>From a practical perspective, it is suggested that a minimum safety distance in metres as the half of vehicle speed measured in kilometres per hour should be attended. In Germany, this is sometimes even obligatory. We introduce a safety distance coefficient c ($c \geq 1$) which is to be understood as a multiplier of the minimum safety distance.

Respecting a discrete speed v ($v = 0, \ldots, v_{\max}$), we have the discrete safety distance:

$$s_{c,v} = \frac{\frac{c}{2} \cdot v \cdot l_c \cdot \frac{1\,\mathrm{h}}{\Delta t} \cdot 10^{-3}}{l_c}. \tag{4}$$

For $\Delta t = 2.4$ s, (4) becomes

$$s_{c,v} = \frac{3cv}{4}. \tag{5}$$

Given a discrete distance d to the immediate leading vehicle, a collision-free speed v requests

$$v + s_{c,v} \leq \frac{d \cdot l_c - l_v}{l_c} = d - \frac{l_v}{l_c}. \tag{6}$$

The safety distance $s_{c,v}$ can be shortened as s_v, if the safety distance coefficient c is clear in the context.

2.3 Driving Strategy

We notice that in the two border lanes lane changing is allowed only in one direction, whereas in the middle lanes lane changing is possible in both directions. Without loss of generality, we consider exactly these three types of lanes and they will be given indices $l = 0, 1, 2$, counted from the inner side. Furthermore,

positions on the lanes $l = 0, 1, 2$ will be written in x, y and z respectively. As in (1b), we use the superscript $'$ to address the immediate leading vehicle in the flow direction: respecting a vehicle at position y, the vehicle directly ahead of it will be at position y'; by x' and z' we mean the positions of the leading vehicles in the neighbouring lanes. In addition, the speed of the vehicle at position x will be written as v_x.

Same as (1a), local vehicle speed will always be increased whenever possible. After this, lane changing will be considered.

Check inner lane This is the case when a vehicle at position y' seeks to change into the inner lane. This step is mandatory in an asymmetric traffic system. Obviously, this driving manoeuvre is only possible when $l > 0$. With

$$x'' - y' - 1 - s_{v_{y'}} \geq v_{y'}, \tag{7a}$$

and

$$v_{y'} > v_x, \tag{7b}$$

a lane changing $\Delta l = -1$ will be possible for the current vehicle with a speed $v_{y'}$. (7a) is the forward causality taking into consideration of safety distance (4). (7b) refers to the backward causality: a higher speed of the current vehicle guarantees a collision-free lane changing.

Check current lane This is the case when the vehicle inspects the situation in the current lane. With

$$y'' - y' - 1 - s_{v_{y'}} \geq v_{y'}, \tag{8}$$

no lane changing will be necessary ($\Delta l = 0$) and the current speed $v_{y'}$ can be maintained. Since no lane changing is involved, backward causality will not be considered, since this will be covered by the forward causality of the immediate following vehicle in the same lane. In an asymmetric traffic system, (8) is generally easier than (7a) to meet, since vehicles in outer lanes usually have higher speeds and consequently the density should be lower, the latter further leads to $y'' - y' > x'' - y'$. This explains why vehicles have no reason to change lanes too often.

Check outer lane Now the current vehicle—still at position y', since the above-mentioned two operations have been without success—seeks to change into the outer lane. To perform this operation, there must be $l < 2$ and

$$z'' - y' - 1 - s_{v_{y'}} \geq v_{y'}, \tag{9a}$$

and

$$y' - z \geq v_{\max}. \tag{9b}$$

In such a case, a lane changing $\Delta l = +1$ can be performed at the current speed $v_{y'}$. In addition to the forward causality (9a), backward causality is now recovered in (9b). We do not request $v_{y'} > v_z$, since a reliable estimate of the speed is difficult with the increasing vehicle speed in the outer lane (in an asymmetric traffic system). Instead, we apply $v_{\max}$ in (9b) to ensure maximum safety.

Move in current lane In the current lane, by (5) (if Δt is configured to be 2.4 s) and (6), the maximum local speed with consideration of safety distance can be deduced:

$$v \Leftarrow \min \left(\frac{4}{4 + 3c} \cdot \left(y'' - y - \frac{l_v}{l_c} \right), v \right). \tag{10}$$

The value of v is in general not an integer. Yet it is still unknown whether the space $y'' - y' - 1$ is sufficient for the current vehicle to move forward in the flow direction. For this, we propose:

$$v \Leftarrow \begin{cases} y'' - y' - 1, & \text{if } v \geq y'' - y' - 1, \\ v^*, & \text{otherwise,} \end{cases}$$

with

$$v^* = \begin{cases} \lfloor v \rfloor + 1, & \text{if } p < v - \lfloor v \rfloor, \\ \lfloor v \rfloor, & \text{otherwise,} \end{cases}$$

where p is a random number from $[0, 1)$ and $\lfloor \cdot \rfloor$ refers to the largest integer no greater than the argument. With the construction of v^*, the position update of the vehicle can be performed exactly.

The above-mentioned four steps refer to the asymmetric case. In a symmetric traffic system, the vehicles are requested—partly owing to the heavy traffic loads—to stay in their lanes whenever possible. On the other side, when a lane changing is necessary, it is allowed on both sides. Hence, lane changing in the symmetric case will be considered on an equal basis; apart from this, another significant change concerns the forward causality (9b), which is to be revised into

$$v_{y'} > v_z.$$

for the sake of symmetric behaviour.

2.4 Space-time diagram

To test our model, periodical boundary of the lanes has been applied. Since the vehicles are now placed in a closed circulating traffic system, the actual physical length of the lanes is no longer relevant for test results. We start with our
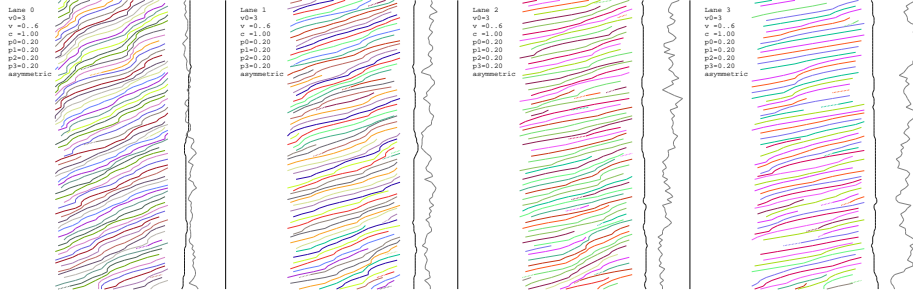
Fig. 2. Space-time diagram of four asymmetric lanes with $p_0 = p_1 = p_2 = p_3 = 0.2$ (standard configuration with minimum safety distance).

standard configuration $l = 15\,\mathrm{m}$, $\Delta t = 2.4\,\mathrm{s}$. Only minimum safety distance is requested ($c = 1$). The vehicles are assigned a default speed of 3 (that is, $67.5\,\mathrm{km} \cdot \mathrm{h}^{-1}$), this initial speed has no significant impact on the overall dynamics of the system, since by (1a), all vehicles are subject to local acceleration whenever possible. The maximum possible speed is set as $v_{\max} = 6$ ($135\,\mathrm{km} \cdot \mathrm{h}^{-1}$).
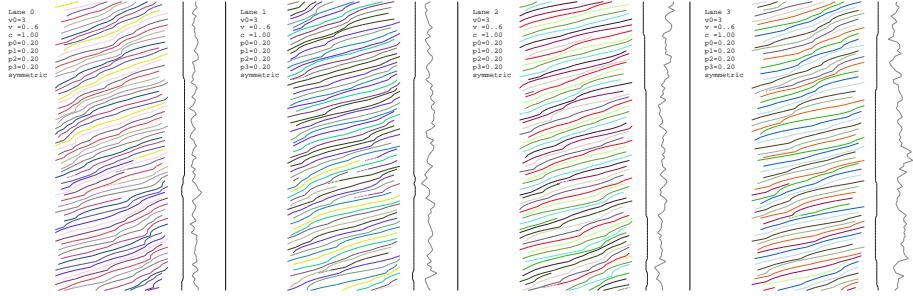

Fig. 3. Space-time diagram of the same settings as above in the symmetric case.

In Fig. 2 and Fig. 3 we see two examples of the so-called *space-time diagram* in which the trajectories of the individual vehicles are recorded. In these two examples, the lanes are initialized with an equal density $p_0 = p_1 = p_2 = p_3 = 0.2$. The average vehicle speed and the vehicle density in the lanes are drawn in gray and black line segments respectively, the straight line segment on the right sight refers to both the maximum speed $v_{\max}$ and the maximum density 1. It can be seen that in the asymmetric case, the average speed increases (accompanied by a slight decrease in the density) in the outer lanes, whereas in the symmetric case, the change of the average speed in the lanes remains small.

3 Model Calibration

3.1 Density and Flow

Now we have a look of the *fundamental diagram* of density and flow, the latter of which is defined as the product of vehicle density and average speed in the lane.
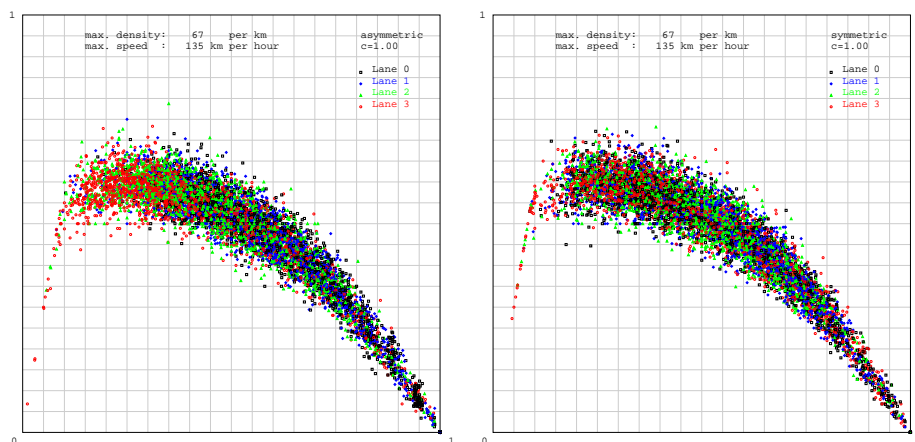

Fig. 4. Sample points of density (horizontal axis) and flow (vertical axis), generated from test runs with various initial lane densities, in both asymmetric and symmetric cases.

Fig. 4 shows the density-flow relationship with standard configuration $l_c = 15$ m, $\Delta t = 2.4$ s and $c = 1$. Naturally, the maximum density "1" in the horizontal axis is given by the inverse of the site length in the lane, that is, $\frac{1}{l_c}$, which is approximately 67 vehicles per kilometre in our case. The maximum flow "1" in the vertical axis refers to the product of maximum density and maximum speed $\frac{v_{max}}{l_c} = \frac{135\,\mathrm{km\cdot h^{-1}}}{15\,\mathrm{m}} = 9000$ vehicles per hour. practically, this maximum flow quantity cannot be realized. Both subfigures exhibit very similar patterns of the generated sample points. They differ in lane distribution of the sample points by definition (asymmetric vs. symmetric).

The same tests can be carried out on a system-wide basis: instead of having density and speed (and consequently flow) measured in separate lanes, we can have these quantities measured over all the lanes. In Fig. 5 we show the test results on a system-wide basis with different safety distance coefficients. Median flow quantities have been collected from sample points in the equidistant intervals respecting density. The speed-flow relationship is given in addition in the right subfigure. In the left subfigure, the maximum flow of over 5000 vehicles per hour is reached at a density of somehow 15 vehicles per kilometre with minimum
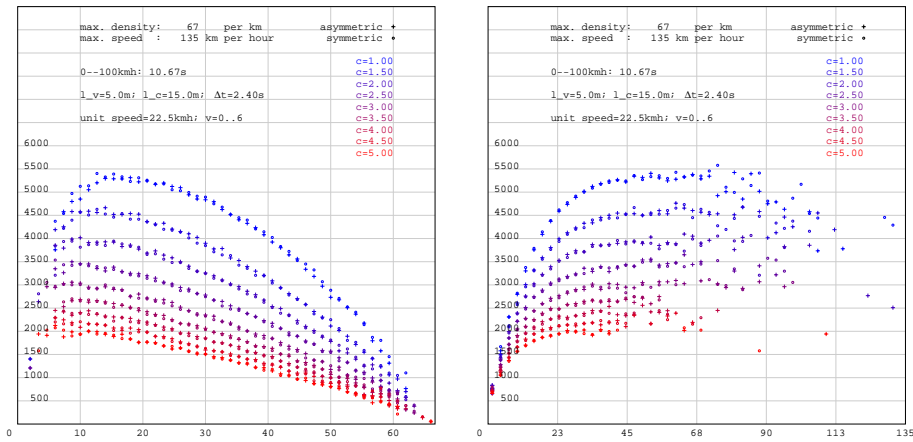
Fig. 5. Fundamental diagram of various safety distance settings in both asymmetric and symmetric cases. Left: Fundamental diagram of density and median flow volume. Right: Diagram of speed and median flow volume. Relative scale is applied with additional labelling of the actual quantities.
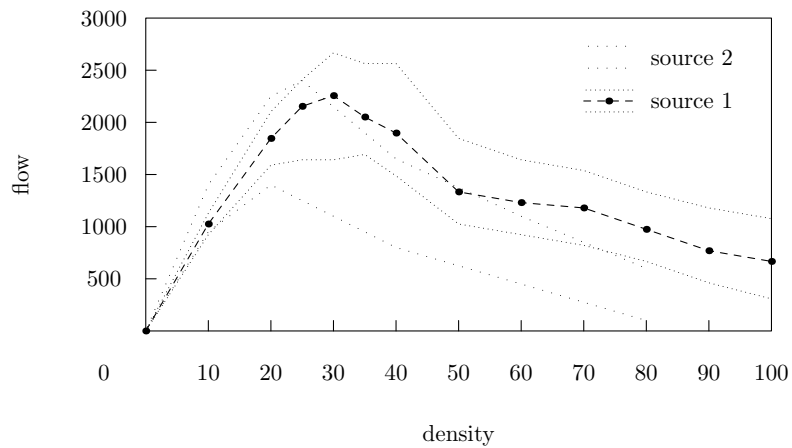

Fig. 6. Re-plot of two fundamental diagrams collected from empirical data concerning two different two-lane highways, both with speed limit $120\,\mathrm{km} \cdot \mathrm{h}^{-1}$. Source 1: [2] (page 87), original sample points are roughly covered in the dotted region, median flow values with various densities are shown in black dots. Source 2: [6], no median flow value had been provided, the original quantities referred to measurements made in two lanes, these have been adjusted in the current plot.

safety distance ($c = 1$).

When the relative scale (with "1" as maximum) is applied, the overall shape of the fundamental diagram of density and flow becomes "flatter" with the increase of the safety distance coefficient c. We also notice that given constant l_v, l_c, Δt and c, the length of the lanes and the discrete maximum speed $v_{\max}$ have no impact on the overall density-flow diagram. $v_{\max}$ affects only the scale in the vertical axis.

In comparison, Fig. 6 presents results acquired from empirical data. There we see an average peak flow of roughly 2300 vehicles per hour at a density of 20 to 30 vehicles per kilometre. Source 2 of Fig. 6 documented that 13% of the recorded vehicles had been trucks (of larger sizes and lower speeds), this would suggest a higher density and flow volume, if only passenger cars were to be considered.
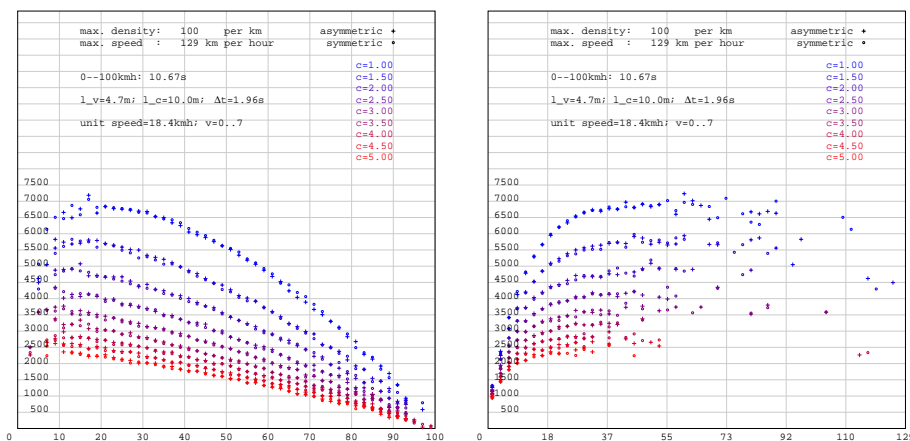
Fig. 7. Fundamental diagram of median flow volume, density and speed with slightly modified parameters. Owing to the rounding of $v_{\max}$, the real speed limit as product of unit speed u and $v_{\max}$ may be higher than the target speed limit $120\,\mathrm{km}\cdot\mathrm{h}^{-1}$.

It is quite reasonable that with $c = 1$, the flow volume would be much higher than expected. Here are two facts. Firstly, drivers usually keep a larger distance to others than the mandatory minimum safety distance; and secondly, the road resources are not at all time completely utilized. On the whole, $c \in [2, 4]$ would be a reasonable range for safety distance coefficient. Before calibrating our model, we adjust two system parameters. We set $l_v = 4.7\,\mathrm{m}$, this represents the average length of a mid-sized passenger and should therefore reflect the average size of the vehicles more exactly; at the same time, in alignment with the empirical data, maximum lane density is now defined to be 100 vehicles per kilometre, this leads to $l_c = 10\,\mathrm{m}$. The result of this configuration is given in Fig. 7. Unlike l_v and l_c, the average acceleration capacity of the vehicles stays unchanged in the test case of Fig. 7, therefore we need to calculate the new Δt (see below). Compared

to empirical data, it seems that in this test case the peak flow is reached too early.
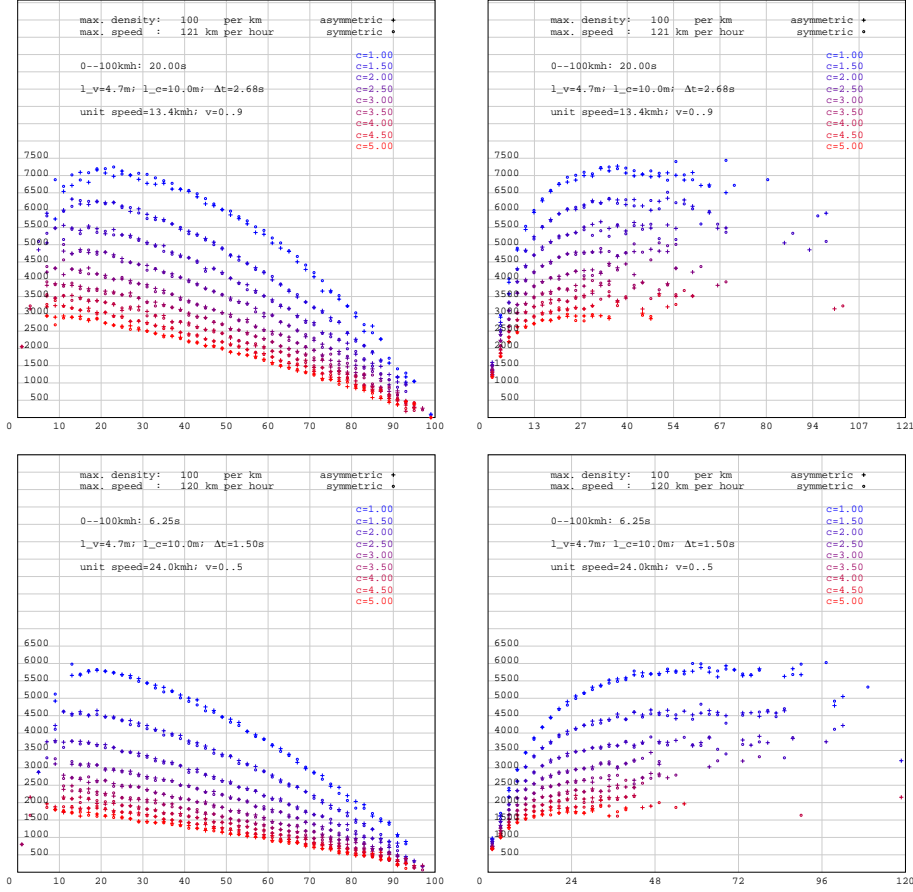
Fig. 8. Fundamental diagrams of median flow volume, density and speed with different values of T. First row: T is larger than that in the standard configuration. Second row: T is reduced to produce the correct flow volume.

Let u denote the real speed associated with the discrete unit speed $v = 1$, we have

$$u = \frac{1\,\mathrm{h}}{\Delta t} \cdot \frac{l_c}{1000\,\mathrm{m}}\,\mathrm{km} \cdot \mathrm{h}^{-1}. \tag{11}$$

Given a target speed limit v_{target} (for example, $v_{\mathrm{target}} = 120\,\mathrm{km} \cdot \mathrm{h}^{-1}$), the maximum discrete speed is

$$v_{\max} = \left\lceil \frac{v_{\mathrm{target}}}{u} \right\rceil. \tag{12}$$

whereas $\lceil \cdot \rceil$ refers to the smallest integer no less than the argument.

Let T denote the time length of acceleration from 0 to $100\,\mathrm{km} \cdot \mathrm{h}^{-1}$ under maximum power, there is

$$T = \frac{100\,\mathrm{km} \cdot \mathrm{h}^{-1}}{\frac{u}{\Delta t}}.$$

By (11), we have

$$\frac{100}{T} = \frac{1\,\mathrm{h}}{(\Delta t)^2} \cdot \frac{l_c}{1000\,\mathrm{m}},$$

this gives

$$\Delta t = \sqrt{\frac{3.6\,\mathrm{s} \cdot l_c \cdot T}{100\,\mathrm{m}}}. \tag{13}$$

Although it may sound strange, increasing T leads to a higher flow volume, since larger T implies weaker acceleration capability of the vehicles. The reason for this is that in the flow diagram with axes of relative scale, the actual flow volume concerning a specific configuration (of l_v, l_c and Δt) is related with the shape (flatness) of the density-flow curve represented by the sample points. As we have pointed out earlier, with a constant configuration, varying $v_{\max}$ has no effect on the shape of the density-flow curve, yet the flow volume changes, since the maximum flow on the vertical axis is the product of maximum density and maximum speed. By (13), we know that Δt is correlated with the square root of T; by (11) and (12), $v_{\max}$ is correlated with Δt. Consequently, with a larger T the actual flow volume increases, this can be verified by the test cases in Fig. 8 as well.

In comparison to our initial configuration of $\Delta t = 2.4\,\mathrm{s}$, $\Delta t = 1.5\,\mathrm{s}$ seems to be quite reasonable (along with modified l_v and l_c) to produce flow volume in a suitable range. However, $\Delta t = 1.5\,\mathrm{s}$ would lead to $T = 6.25\,\mathrm{s}$ which represents a much too high acceleration capacity, see the second test case in Fig. 8. As a solution for this, we introduce an additional acceleration multiplier s $(s > 1)$ that the vehicle should have a simulated acceleration capacity from 0 to $100\,\mathrm{km} \cdot \mathrm{h}^{-1}$ in a time length of Ts. To achieve this, we request that (1a) will be carried out with a probability of q_v, for $v = 0, \ldots, v_{\max} - 1$. Translated into discrete form, the acceleration from $v = 0$ to $v = v_{\max}$ should then take $v_{\max} \cdot s$ steps, that is
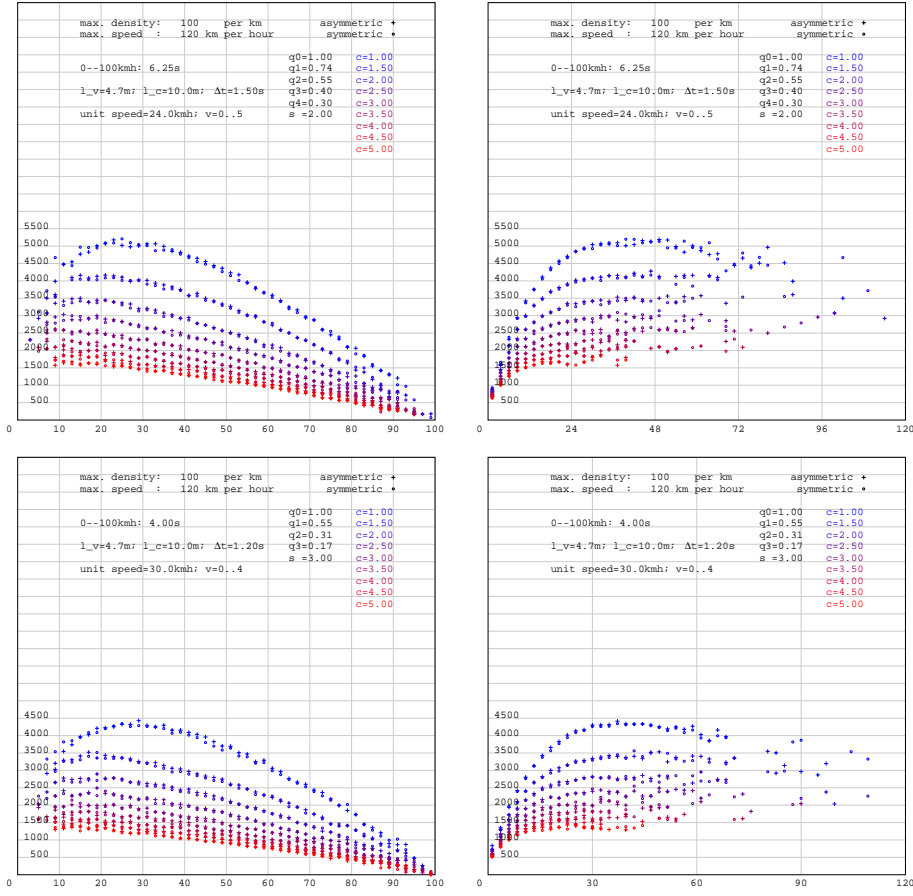
$$\sum_{i=0}^{v_{\max}-1} \frac{1}{q_i} = v_{\max} \cdot s. \tag{14}$$

In the trivial case $v_{\max} = 1$ we may set: $q_0 = \frac{1}{s}$. Otherwise, we request

$$q_0 = 1, \tag{15}$$
$$q_{i+1} = q_i \cdot q, \quad \text{for } i = 0, \ldots, v_{\max} - 2. \tag{16}$$

(15) says that acceleration from a stationary state will always be carried out (apart from the trivial case); and with (16), acceleration decays with a probability q $(0 < q < 1)$. With the solution of (14), postponed acceleration can be

12

Fig. 9. Calibrated diagrams of median flow volume, density and speed with additional acceleration multipliers.

simulated. Two further test cases are shown in Fig. 9. For the configuration of $T = 6.25\,\text{s}$ and $s = 2$, $c = 3$ or 3.5 seems to produce maximum flow volume in the range of 2300 to 2600 vehicles per hour; for $T = 4\,\text{s}$ and $s = 3$, $s = 2.5$ gives the maximum flow volume of approximately 2300 per hour at a density slightly above 20 vehicles per kilometre. These two parameter settings represent a reasonable acceleration capacity (0 to $100\,\text{km}\cdot\text{h}^{-1}$ in 12 and 12.5 seconds respectively) and at the same time, v_{max} in (12) has integer solution.

Acknowledgement

References

1. M.-J. Chen, G. Bärwolff, and H. Schwandt. A deductive model for multi-lane vehicular traffic. In *18th IEEE International Conference on Intelligent Transportation Systems*, pages 900–905, 2015.
2. D. Helbing. *Verkehrsdynamik: Neue physikalische Modellierungskonzepte*. Springer-Verlag Berlin Heidelberg, 1997. ISBN 978-3-642-63834-3.
3. S. P. Hoogendoorn and P. H. L. Bovy. State-of-the-art of vehicular traffic flow modelling. Proceedings of the Institution of Mechanical Engineers, Part I: *Journal of Systems and Control Engineering*, 215(4): 283–303, 2001.
4. A. Kesting, M. Treiber, and D. Helbing. Agents for traffic simulation. In A. Uhrmacher and D. Weyns, editors, *Multi-Agent Systems: Simulation and Applications*, pages 325–356, CRC Press, 2009. ISBN 978-1-4200-6023-1.
5. K. Nagel and M. Schreckenberg. A cellular automaton model for freeway traffic. *J. Phys. I France*, 2:2221–2229, 1992.
6. K. Nagel, D. E. Wolf, P. Wagner, and P. Simon. Two-lane traffic rules for cellular automata: A systematic approach. *Physical Review E*, 58(2):1425–1437, 1998.
7. M. Rickert, K. Nagel, M. Schreckenberg, and A. Latour. Two lane traffic simulations using cellular automata. *Physica A*, 231:534–550, 1996.
8. M. Treiber and A. Kesting. *Traffic Flow Dynamics*. Springer-Verlag Berlin Heidelberg, 2013. ISBN 978-3-642-32459-8.